JOURNAL OF
CHEMICAL &
ENGINEERING
DATA

Article

pubs.acs.org/jced

Adsorption Equilibrium of Thiophenic Sulfur Compounds on the Cu-BTC Metal−Organic Framework

Baojian Liu,* Yinbang Zhu, Shiwang Liu, and Jianwei Mao

School of Biological and Chemical Engineering, Zhejiang University of Science and Technology, Hangzhou, Zhejiang, China 310023

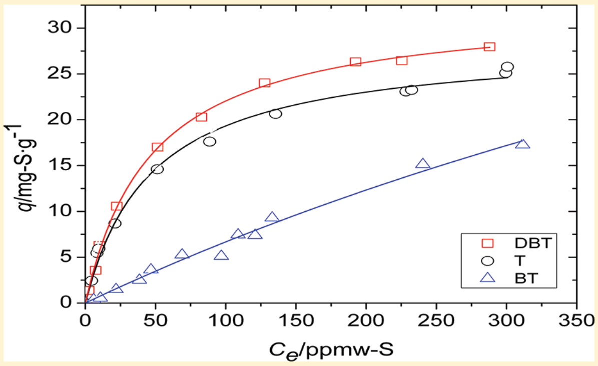

ABSTRACT: Thiophenic compounds are the refractory organosulfur compounds remaining in the transportation fuels, and their removal from liquid fuels has become increasingly important. In this work, adsorption isotherms of thiophene (T), benzothiophene (BT), and dibenzothiophene (DBT) in isooctane onto a metal−organic framework (Cu-BTC) were measured for (293.15 to 313.15) K and equilibrium sulfur concentrations up to 370 ppmw-S (ppmw of sulfur). The adsorption capacity followed the order of BT < T < DBT under the investigated sulfur concentrations and temperatures. The adsorption isotherms of T and DBT are highly favorable. The isotherm data were well-correlated using a multitemperature Langmuir model, and three parameters were extracted for each thiophenic compound. The multitemperature Langmuir model has predictive ability for the adsorption of T, BT, and DBT within the sulfur concentration range and the temperature range studied. The heat of adsorption (Δ*H*) of T, BT, and DBT is (−21.99, −14.23, and −37.34) kJ·mol^{-1}, respectively. The order of Δ*H* is in agreement with the adsorption affinities.

■ INTRODUCTION

Thiophenic compounds are naturally present in crude oils and also in transportation fuels. During combustion of sulfur-containing fuels, the sulfur compounds are converted to SO_x, which is the main source of acid rain. Sulfur in fuels will poison the catalysts in catalytic converters of vehicles, which are used to remove pollutants such as NO_x and particulate matter from engine exhaust. Therefore, the demand of low-sulfur gasoline and diesel is increasing, and increasingly stringent government regulations are mandated. The European Union has mandated the reduction of sulfur contents in gasoline and diesel fuels to 10 ppmw by 2009, and the U.S. EPA (U.S. Environmental Protection Agency) stipulated that ultralow sulfur diesel (ULSD) with sulfur concentrations lower than 15 ppmw should be used by 2010.[1]

The removal of sulfur-containing compounds from fuels in a petroleum refinery is carried out by the hydrodesulfurization (HDS) process. HDS is highly efficient for the removal of thiols, sulfides, and disulfides, but less effective for thiophene (T), benzothiophene (BT), dibenzothiophene (DBT) and their derivatives.[2] Thus, the organosulfurs remaining in gasoline or diesel fuels are mainly T, BT, DBT, and their derivatives. Due to the low reactivity of thiophenic compounds, it is extremely costly and requires high operating temperature and pressure to reduce the sulfur content to less than 10 ppmw by existing HDS technology. The removal of the refractory sulfur compounds in the fuels after the conventional HDS processes by adsorption is a promising way to produce ultralow sulfur fuels. The adsorption process is usually carried out under mild conditions, and it can be potentially used in industrial desulfurization.

Selective adsorption of thiophenic compounds from transportation fuels has attracted particular interest during the past decade. Various types of adsorbents such as zeolites,[3−7] activated carbons,[8−13] metal oxides,[14] and other mesoporous materials[15,16] have been investigated. Among them, most of the adsorbents were modified by metal ions based on the π-complexation. Yang and his co-workers[3,4] reported that the Ag^+ or Cu^+ exchanged Y-zeolites based on π-complexation were capable of producing fuels with sulfur content lower than 10 ppmw or even no sulfur fuels by using model fuels, but Cu(I)-Y is less effective for commercial fuels and not highly stable as it can be oxidized easily into Cu(II)-Y, which has a weaker π-complexation effect. So far, it is still a challenge for the industrial production of low-sulfur fuels using adsorption technology.

Metal−organic frameworks (MOFs), which consist of clusters or chains of metal ions connected by organic linkers, are a new class of inorganic−organic hybrid porous materials. MOFs have extra-high specific surface areas, highly ordered pore structures, and easy tenability of pore size and shape. MOFs are more versatile for application-oriented tailing than activated carbons and zeolites. MOFs have been frequently investigated for gas storage, gas separation, and catalysis.[17] Recently, MOFs have been shown to remove thiophenic compounds from model fuels,[1,18−23] which represents a type of alternative adsorbents for cost-effective production of low-sulfur fuels by selective adsorption. However, the adsorption behavior of thiophenic

Received: January 29, 2012
Accepted: February 27, 2012
Published: March 6, 2012

dx.doi.org/10.1021/je300130s | *J. Chem. Eng. Data* 2012, 57, 1326−1330

compounds on MOFs has not been extensively studied. The thermodynamic effect of thiophenic compound adsorption onto MOFs has not been reported.

In this work, we comprehensively describe the adsorption isotherms of T, BT, and DBT in model liquid fuels on a commercially available MOF Cu-BTC under (293.15 to 313.15) K and up to 370 ppmw-S (ppmw of sulfur) equilibrium sulfur concentration. Adsorption isotherm data were correlated well using a multitemperature Langmuir model, and the model parameters were determined for each thiophenic compound. The multitemperature Langmuir model has the advantages of fewer parameters and predictive ability for adsorption of any sulfur concentration of T, BT, and DBT at any temperature within the sulfur concentration range and the temperature range studied.

■ EXPERIMENTAL SECTION

Materials. T (mass fraction purity of 0.99), BT (mass fraction purity of 0.98), and DBT (mass fraction purity of 0.98) were supplied by J&K Scientific Ltd. (Shanghai, China). Isooctane (mass fraction purity of 0.997) was purchased from Scharlab, S.L. (Shanghai, China). The MOF Cu-BTC was supplied by Sigma-Aldrich (Beijing, China) in powder form under the trade name of Basolite C300. Prior to adsorption, the sample was evacuated under vacuum at 443.15 K for 24 h to make sure that the sample was totally activated.

Model Sulfur Solution. In this study, model sulfur solutions were prepared by independently adding T, BT, or DBT to liquid isooctane with different initial concentrations ranging from (10 to 630) ppmw of sulfur (the initial concentrations of T, BT, and DBT were in the range of (1.207 to 19.67) mmol·kg^{-1}, (0.325 to 17.42) mmol·kg^{-1}, and (0.551 to 19.22) mmol·kg^{-1}, respectively).

Adsorption Procedure. The adsorption equilibrium experiments were conducted at three different temperatures from (293.15 to 313.15) K using a temperature-controlled shaker. The amount, (40 to 60) mg, of C300, after activation pretreatment, was weighed and mixed in tubular vials (10 cm^3 volume) with 5 cm^3 of the sulfur-containing solution with different initial concentrations ranging from (10 to 630) ppmw-S. All solutions were prepared in isooctane. The vials were then sealed and shaken at 200 rpm in a temperature-controlled shaker for 24 h at constant temperature, which was confirmed to be sufficient to reach adsorption equilibrium. After adsorption equilibrium, the solutions were separated from the adsorbents with a syringe filter (PTFE, hydrophobic, 0.25 μm). The solute concentrations in the filtrates were analyzed by a Waters e2695 high-performance liquid chromatograph (HPLC) equipped with a Waters 2489 UV–vis detector and an ODS-C$_{18}$ column. The mobile phase was (90 + 10) cm^3 (methanol + water), and the flow rate was 1.0 cm^3·min^{-1}; the ODS-C$_{18}$ column was maintained at 308.15 K. T, BT, and DBT were detected at 220 nm, 254 nm, and 330 nm, respectively. The amount adsorbed was calculated by the material balance:

$$q = \frac{\rho V(C_0 - C_e)}{m} \tag{1}$$

where q is the amount adsorbed (mmol·g^{-1}), V is the volume of the liquid solution (cm^3), ρ is the density of isooctane (6.9·10^{-4} kg·cm^{-3}), C_0 and C_e are the initial and equilibrium solute concentrations in solution (mmol·kg^{-1}), and m is the mass of adsorbent (g).

■ RESULTS AND DISCUSSION

Characterization of Adsorbent. Cu-BTC (also known as HKUST-1) framework has paddlewheel type metal corners connected by benzene-1,3,5-tricarboxylate (BTC) linkers. Each metal corner has two copper atoms bonded to the oxygen of four BTC linkers. According to the supplier, the commercial Cu-BTC (Basolite C300) has a Brunauer–Emmett–Teller (BET) surface area of (1500 to 2100) m^2·g^{-1}.[24] In this work, the activated Cu-BTC samples were characterized by volumetric N$_2$ adsorption/desorption isotherms at 77 K by a Quantachrome NOVA 4200e surface area and pore size analyzer using N$_2$ with a mass fraction purity of 99.999 (Cryogenic Gases). The specific surface area was evaluated by means of the BET method and Langmuir method. The measured BET and Langmuir surface areas are (1614 and 1869) m^2·g^{-1}, respectively. The properties of C300 are presented in Table 1.

Table 1. Properties of the Commercial Cu-BTC Metal–Organic Framework

property	Cu-BTC
commercial name	Basolite C300
supplier	Sigma-Aldrich
activation conditions	443.15 K, 24 h
particle size	15.96 μm (D50)
bulk density	0.35 g·cm^{-3}
BET surface area	1614 m^2·g^{-1}
Langmuir surface area	1869 m^2·g^{-1}

Adsorption Equilibrium Data. The original adsorption equilibria data of T, BT, and DBT at (293.15 to 313.15) K are presented in Table 2. Cu-BTC exhibits tremendous capacities for DBT and high capacities for T even when the liquid phase equilibrium concentrations are very low, while BT has much lower adsorption capacities on Cu-BTC. Khan et al.[23] measured the adsorption of BT in *n*-octane onto MIL-53(Al), MIL-53(Cr), and MIL-47 at (298.15, 308.15, and 318.15) K; the adsorption capacity follows the order of MIL-53(Al) < MIL-53(Cr) < MIL-47. Comparing Khan et al.'s adsorption isotherms of BT with Table 2 of this work, Cu-BTC has higher adsorption capacity of BT than MIL-53(Al) and MIL-53(Cr), but lower capacity than MIL-47. For example, at a 2.1555 mmol-BT·kg^{-1} equilibrium concentration, Cu-BTC has an adsorption capacity of 0.164 mmol-BT·g^{-1} at 293.15 K; MIL-53(Al), MIL-53(Cr), and MIL-47 have approximately (0.052, 0.119, and 0.373) mmol-BT·g^{-1} at 298.15 K, respectively.

To compare with government regulations and literature results, the concentrations of liquid in mmol·kg^{-1} were converted to ppmw-S, and the amounts adsorbed in mmol·g^{-1} were converted to mg-S·g^{-1} by multiplying by 32, where 32 is the molecular weight of sulfur. Figure 1 shows the adsorption equilibrium of T, BT, and DBT on Cu-BTC at 293.15 K. The adsorption affinity was observed to follow the order of DBT > T > BT. DBT and T have much higher adsorption capacities than BT over the concentration range investigated. It has been demonstrated that Cu-BTC has higher adsorption capacities for T and DBT and lower capacity for BT than the Cu(I)-Y zeolite. For example, at 293.15 K and 80 ppmw-S, Cu-BTC has adsorption capacities of (17.89, 5.40, and 20.41) mg-S·g^{-1} for T, BT, and DBT, respectively. In comparison, Cu(I)-Y zeolite has capacities of (10.52, 32.2, and 18.91) mg-S·g^{-1} for T, BT, and DBT, respectively.[7]

Table 2. Adsorption Isotherm Data of Thiophenic Compounds on Metal−Organic Framework Cu-BTC Based on Solute Concentrations

T		BT		DBT	
C_e	q	C_e	q	C_e	q
mmol·kg^{-1}	mmol·g^{-1}	mmol·kg^{-1}	mmol·g^{-1}	mmol·kg^{-1}	mmol·g^{-1}
293.15 K		293.15 K		295.15 K	
0.1397	0.0764	0.1861	0.0118	0.0773	0.0429
0.2606	0.1706	0.3364	0.0170	0.2293	0.1116
0.3019	0.1855	0.6846	0.0461	0.3144	0.1961
0.6607	0.2712	1.2048	0.0782	0.7010	0.3304
1.6045	0.4562	1.4601	0.1136	1.6116	0.5320
2.7691	0.5502	2.1555	0.1643	2.5851	0.6342
4.2357	0.6451	3.0273	0.1596	3.9919	0.7505
7.1359	0.7216	3.4015	0.2310	6.0145	0.8228
7.2636	0.7264	3.7800	0.2328	7.0448	0.8266
9.3546	0.7844	4.1607	0.2904	8.9981	0.8739
9.3926	0.8054	7.5113	0.4725		
		9.7317	0.5393		
		303.15 K			
0.1759	0.0784	0.1849	0.0100	0.0929	0.0412
0.3433	0.1676	0.3223	0.0158	0.2504	0.1042
0.7523	0.2482	0.7290	0.0402	0.4994	0.2046
2.0428	0.4558	1.1865	0.0805	0.7033	0.2887
3.0262	0.5304	1.7532	0.0942	2.2945	0.4732
4.8396	0.6392	2.9883	0.1431	2.9474	0.5951
7.7399	0.7021	3.3917	0.1940	3.0875	0.6495
8.0779	0.7124	4.7588	0.2461	4.4448	0.7049
8.6197	0.7471	5.3223	0.2732	8.3239	0.7522
8.9233	0.7520	7.5816	0.3756	10.8019	0.8125
10.7729	0.7400	10.4646	0.4513		
		10.9117	0.4708		
		313.15 K			
0.2433	0.0724	0.1622	0.0103	0.1670	0.0425
0.4193	0.1488	0.2888	0.0169	0.3001	0.1040
1.1317	0.2561	0.5938	0.0383	0.6419	0.1917
2.4948	0.4424	1.4719	0.0724	1.5871	0.2909
3.0469	0.4811	1.7986	0.0953	3.0120	0.4399
4.8620	0.5801	2.6552	0.1460	5.4215	0.6185
7.9383	0.6569	4.2526	0.1871	7.0196	0.6794
8.8406	0.6405	4.2623	0.2033	9.1312	0.7245
9.0407	0.6807	5.0812	0.2490	11.6533	0.7908
10.0052	0.7296	5.3807	0.2484		
10.7126	0.6918	8.1744	0.3589		
		11.0317	0.4108		

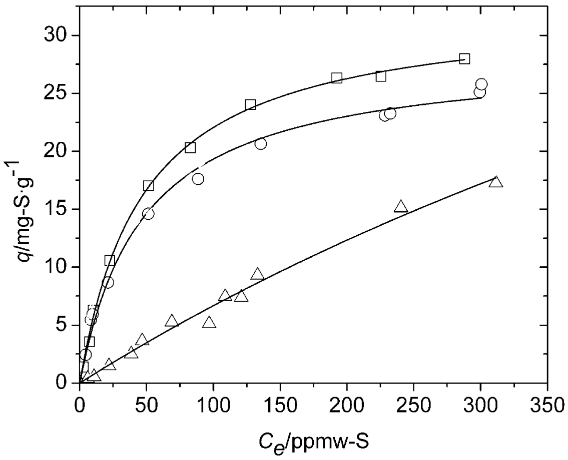

Figure 1. Adsorption isotherms of T, BT, and DBT on Cu-BTC: □, DBT at 295.15 K; ○, T at 293.15 K; △, BT at 293.15 K; the solid lines are the Langmuir isotherm.

Analysis of Adsorption Isotherm Models. The simplest and most commonly used Langmuir (eq 2) and Freundlich (eq 3) isotherm models were used to correlate the experimental isotherm data. The equations are as follows

$$q = \frac{q_m b C_e}{1 + bC_e} \tag{2}$$

$$q = kC_e^n \tag{3}$$

The Freundlich isotherm only gave a good fit to BT while resulting in a significantly worse correlation for T and DBT. The Langmuir isotherm model provided much better fits than the Freundlich model and yielded good correlations to T, BT, and DBT. At different temperatures, the measured isotherm data of all thiophenic compounds were fitted independently with the Langmuir model. The results of the fitting procedure by nonlinear least-squares regression analysis are summarized in Table 3. As is indicated by the correlation coefficients, the Langmuir model gave a good fit for all the conditions. The experimental and Langmuir isotherm model correlated adsorption isotherms of thiophenic compounds on Cu-BTC at varying temperatures are illustrated in Figures 2 to 4. All of the adsorption isotherms of T and DBT are very favorable, while those of BT are somewhat linear.

The adsorption equilibrium data of T, BT, and DBT at three temperatures can be correlated very well by the Langmuir isotherm. As shown in Table 3, the values of q_m and b are both temperature-dependent for T, BT, and DBT. To evaluate the temperature effect on the adsorption and estimate the thermodynamic parameters, we tried to fit the adsorption equilibrium data of each thiophenic compound by the multitemperature Langmuir model, which considers q_m to be independent of temperature.

Therefore, for each thiophenic compound, a total of four parameters including a temperature-independent q_m and three temperature-dependent b were used to optimize simultaneously. The parameters were obtained by minimizing the sum of squared deviations between the experimental data at three temperatures and the calculated values, which was performed by nonlinear regression through a Matlab code. The best fitting curves for T, BT, and DBT are shown in Figures 2 to 4. It is obvious that the experimental data are described well by the multitemperature Langmuir model for T, BT, and DBT at all temperautures. The best fitted values of q_m and b for T, BT, and DBT are presented in Table 3.

As shown in Table 3, when the temperature increased, the Langmuir equilibrium constant b decreased. The temperature dependency of the Langmuir equilibrium constant can generally be expressed by the Arrhenius equation as follows[25,26]

$$b = b_0 \exp\left(-\frac{\Delta H}{RT}\right) \tag{4}$$

where b_0 is the pre-exponential factor; R (8.314 J·mol^{-1}·K^{-1}) is the gas constant; T (K) is the temperature, and ΔH is the heat of adsorption. The Arrhenius plot (ln b vs T^{-1}) is illustrated in Figure 5, b_0 and ΔH were obtained through the y-intercept and the slope of the Arrhenius plot, respectively. The resulting values of b_0 and ΔH are presented in Table 3. The negative values of ΔH imply that the adsorption of thiophenic

Table 3. Parameters of the Individual and Multitemperature Langmuir Models for the Adsorption of Thiophenic Compounds on Cu-BTC

	Individual Langmuir				Multitemperature Langmuir			
	T	q_m	b		q_m	b	b_0	ΔH
sorbate	K	mg-S·g^{-1}	(ppmw-S)$^{-1}$	R^2	mg-S·g^{-1}	(ppmw-S)$^{-1}$	(ppmw-S)$^{-1}$	kJ·mol^{-1}
T	293.15	28.456	0.02115	0.994	28.12	0.02186	$2.634\cdot10^{-6}$	−21.99
	303.15	28.348	0.01661	0.997		0.01654		
	313.15	27.500	0.01294	0.995		0.01227		
BT	293.15	81.206	0.00089	0.989	60.95	0.00127	$3.581\cdot10^{-6}$	−14.23
	303.15	51.188	0.00120	0.997		0.00096		
	313.15	38.531	0.00152	0.995		0.00088		
DBT	295.15	32.482	0.02113	0.999	32.09	0.02191	$5.446\cdot10^{-9}$	−37.34
	303.15	30.134	0.01791	0.991		0.01523		
	313.15	32.992	0.00843	0.996		0.00922		

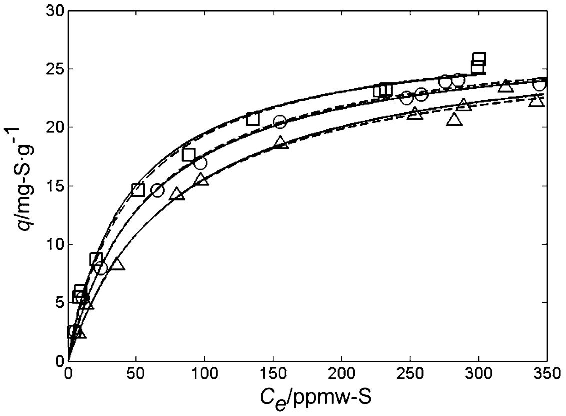

Figure 2. Adsorption isotherms for T on Cu-BTC showing a comparison between the experimental data and the Langmuir isotherm models: □, 293.15 K; ○, 303.15 K; △, 313.15 K; the solid lines are the multitemperature Langmuir model, and the dotted lines are the individual Langmuir model.

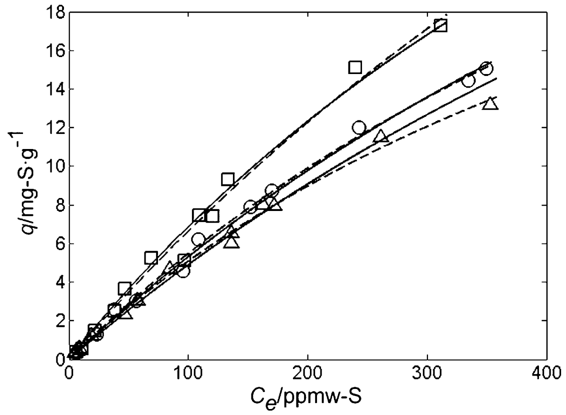

Figure 3. Adsorption isotherms for BT on Cu-BTC showing a comparison between the experimental data and the Langmuir isotherm models: □, 293.15 K; ○, 303.15 K; △, 313.15 K; the solid lines are the multitemperature Langmuir model, and the dotted lines are the individual Langmuir model.

compounds onto Cu-BTC is an exothermic process. As shown in Table 3, the absolute value of ΔH follows DBT > T > BT, which suggests that DBT has the highest adsorption affinity while BT has the lowest adsorption affinity. The order of ΔH is in good agreement with the adsorption capacities of T, BT, and DBT.

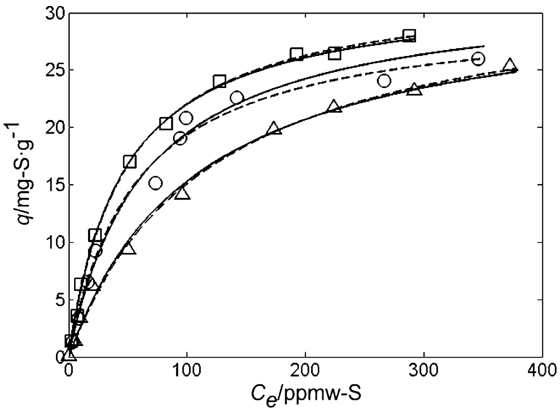

Figure 4. Adsorption isotherms of DBT on Cu-BTC showing a comparison between the experimental data and the Langmuir isotherm models: □, 295.15 K; ○, 303.15 K; △, 313.15 K; the solid lines are the multitemperature Langmuir model, and the dotted lines are the individual Langmuir model.

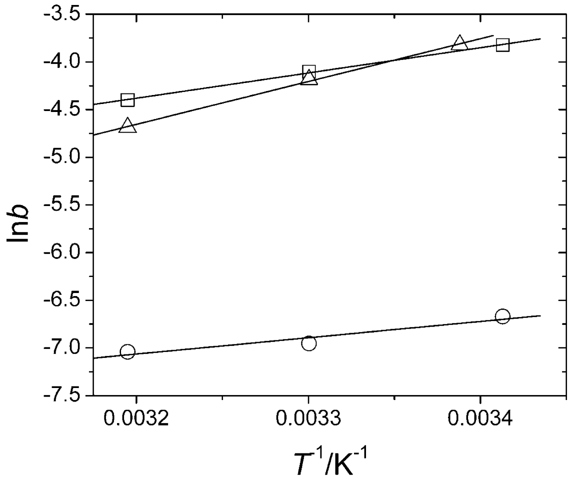

Figure 5. Arrhenius plot showing the temperature dependence of the Langmuir equilibrium constants (b) of thiophenic compounds adsorption on Cu-BTC: □, T; △, DBT; ○, BT.

By coupling eq 2 with eq 4, the multitemperature Langmuir model is expressed as

$$q = \frac{q_m b_0 \exp(-\Delta H/RT)\cdot C_e}{1 + b_0 \exp(-\Delta H/RT)\cdot C_e} \tag{5}$$

Therefore, with the obtained q_m, b_0, and ΔH, the multitemperature Langmuir model has advantages of fewer parameters and predictive ability for adsorption of T, BT, and DBT at any temperature within the sulfur concentration range and the temperature range studied.

■ CONCLUSION

The single-solute adsorption equilibria of T, BT, and DBT in isooctane onto the Cu-BTC MOF were measured in the temperature range of (293.15 to 313.15) K and the equilibrium liquid-phase sulfur concentrations up to 370 ppmw-S. The adsorption capacity of thiophenic compounds onto Cu-BTC follows the order of DBT > T > BT. The adsorption isotherms of T and DBT are highly favorable, while the isotherms of BT are less favorable and somewhat linear under all of the temperatures studied. The Langmuir model with temperature-dependent q_m and the multitemperature Langmuir model with temperature-independent q_m were both successfully used to correlate all of the isotherm data of thiophenic compounds at various temperatures. The entire isotherm data of T, BT, and DBT have been described well by the multitemperature Langmuir model, which uses three parameters to describe the isotherms at different temperatures. The heat of adsorption (ΔH) of T, BT, and DBT is (−21.99, −14.23, and −37.34) $\text{kJ}\cdot\text{mol}^{-1}$, respectively. The order of ΔH is in agreement with the adsorption affinities of thiophenic compounds on Cu-BTC.

■ AUTHOR INFORMATION

Corresponding Author

*Tel.: +86 571 8507 0375. Fax: +86 571 8507 0378. E-mail: baojian_liu@126.com.

Funding

This work was supported by the Zhejiang Provincial Natural Science Foundation of China (Grant No. Y4100189).

Notes

The authors declare no competing financial interest.

■ REFERENCES

(1) Achmann, S.; Hagen, G.; Hammerle, M.; Malkowsky, I.; Kiener, C.; Moos, R. Sulfur Removal from Low-Sulfur Gasoline and Diesel Fuel by Metal-Organic Frameworks. *Chem. Eng. Technol.* **2010**, *33*, 275−280.

(2) Song, C. S. An overview of new approaches to deep desulfurization for ultra-clean gasoline, diesel fuel and jet fuel. *Catal. Today* **2003**, *86*, 211−263.

(3) Yang, R. T.; Hernandez-Maldonado, A. J.; Yang, F. H. Desulfurization of Transportation Fuels with Zeolites under Ambient Conditions. *Science* **2003**, *301*, 79−81.

(4) Hernandez-Maldonado, A. J.; Yang, R. T. Desulfurization of Transportation Fuels by Adsorption. *Catal. Rev.* **2004**, *46*, 111−150.

(5) Wang, H. G.; Song, L. J.; Jiang, H.; Xu, J.; Jin, L. L.; Zhang, X. T.; Sun, Z. L. Effects of olefin on adsorptive desulfurization of gasoline over Ce(IV)Y zeolites. *Fuel Process. Technol.* **2009**, *90*, 835−838.

(6) Shan, J. H.; Liu, X. Q.; Sun, L. B.; Cui, R. Cu-Ce Bimetal Ion-Exchanged Y Zeolites for Selective Adsorption of Thiophenic Sulfur. *Energy Fuels* **2008**, *22*, 3955−3959.

(7) Ma, L. P.; Yang, R. T. Selective Adsorption of Sulfur Compounds: Isotherms, Heats, and Relationship between Adsorption from Vapor and Liquid Solution. *Ind. Eng. Chem. Res.* **2007**, *46*, 2760−2768.

(8) Xiao, J.; Bian, G. A.; Zhang, W.; Li, Z. Adsorption of Dibenzothiophene on Ag/Cu/Fe-Supported Activated Carbons Prepared by Ultrasonic-Assisted Impregnation. *J. Chem. Eng. Data* **2010**, *55*, 5818−5823.

(9) Zhou, A. N.; Ma, X. L.; Song, C. S. Effects of oxidative modification of carbon surface on the adsorption of sulfur compounds in diesel fuel. *Appl. Catal. B: Environ.* **2009**, *87*, 190−199.

(10) Seredych, M.; Lison, J.; Jans, U.; Bandosz, T. J. Textural and chemical factors affecting adsorption capacity of activated carbon in highly efficient desulfurization of diesel fuel. *Carbon* **2009**, *47*, 2491−2500.

(11) Yang, Y.; Ku, H.; Ying, P.; Jiang, Z.; Li, C. Selective dibenzothiophene adsorption on modified activated carbons. *Carbon* **2007**, *45*, 3042−3059.

(12) Yu, M. X.; Li, Z.; Ji, Q. N.; Wang, S. W.; Su, D. G.; Lin, Y. S. Effect of thermal oxidation of activated carbon surface on its adsorption towards dibenzothiophene. *Chem. Eng. J.* **2009**, *148*, 242−247.

(13) Zou, A.; Ma, X.; Song, Ch. Liquid-phase adsorption of multi-ring thiophenic sulfur compounds on carbon materials with different surface properties. *J. Phys. Chem. B* **2006**, *110*, 4699−4707.

(14) Huang, L. C.; Qin, Z. F.; Wang, G. F.; Du, M. X.; Ge, H.; Li, X. K.; Wu, Z. W.; Wang, J. G. A detailed study on the negative effect of residual sodium on the performance of Ni/ZnO adsorbent for diesel fuel desulfurization. *Ind. Eng. Chem. Res.* **2010**, *49*, 4670−4675.

(15) Dai, W.; Zhou, Y. P.; Li, S. N.; Li, W.; Su, W.; Sun, Y.; Zhou, L. Thiophene Capture with Complex Adsorbent SBA-15/Cu(I). *Ind. Eng. Chem. Res.* **2006**, *45*, 7892−7896.

(16) Li, W. L.; Tang, H.; Zhang, T.; Li, Q.; Xing, J. M.; Liu, H. Z. Ultra-deep desulfurization adsorbents for hydrotreated diesel with magnetic mesoporous aluminosilicates. *AIChE J.* **2010**, *56*, 1391−1396.

(17) Czaja, A.; Trukhan, N.; Muller, U. Industrial application of metal-organic frameworks. *Chem. Soc. Rev.* **2009**, *38*, 1284−1293.

(18) Blanco-Brieva, G.; Campos-Martin, J. M.; Al-Zahrani, S. M.; Fierro, J. L. G. Effectiveness of metal-organic frameworks for removal of refractory organo-sulfur compound present in liquid fuels. *Fuel* **2011**, *90*, 190−197.

(19) Shi, F.; Hammoud, M.; Thompson, L. T. Selective adsorption of dibenzothiophene by Functionalized metal organic framework sorbents. *Appl. Catal. B: Environ.* **2011**, *103*, 261−265.

(20) Cychosz, K. A.; Wong-Foy, A. G.; Matzger, A. J. Liquid Phase Adsorption by Microporous Coordination Polymers: Removal of Organosulfur Compounds. *J. Am. Chem. Soc.* **2008**, *130*, 6938−6939.

(21) Cychosz, K. A.; Wong-Foy, A. G.; Matzger, A. J. Enabling Cleaner Fuels: Desulfurization by Adsorption to Microporous Coordination Polymers. *J. Am. Chem. Soc.* **2009**, *131*, 14538−14543.

(22) Park, T. H.; Cychosz, K. A.; Wong-Foy, A. G.; Dailly, A.; Matzger, A. J. Gas and liquid phase adsorption in isostructural $\text{Cu}_3[\text{biaryltricarboxylate}]_2$ microporous coordination polymers. *Chem. Commun.* **2011**, *47*, 1452−1454.

(23) Khan, N. A.; Jun, J. W.; Jeong, J. H.; Jhung, S. H. Remarkable adsorption performance of a metal-organic framework, vanadium-benzenedicarboxylate (MIL-47), for benzothiophene. *Chem. Commun.* **2011**, *47*, 1306−1308.

(24) Lamia, N.; Jorge, M.; Granato, M. A.; Almeida Paz, F. A.; Chevreau, H.; Rodrigues, A. E. Adsorption of propane, propylene and isobutane on a metal-organic framework: Molecular simulation and experiment. *Chem. Eng. Sci.* **2009**, *64*, 3246−3259.

(25) Nam, H. G.; Park, K. M.; Lim, S. S.; Mun, S. Y. Adsorption Equilibria of Succinic Acid and Latic Acid on Amberchrom CG300C Resin. *J. Chem. Eng. Data* **2011**, *56*, 464−471.

(26) Aprea, P.; Caputo, D.; Gargiulo, N.; Iucolano, F.; Pepe, F. Modeling Carbon Dioxide Adsorption on Microporous Substrates: Comparison between Cu-BTC Metal-Organic Framework and 13X Zeolitic Molecular Sieve. *J. Chem. Eng. Data* **2010**, *55*, 3655−3661.